

Cyclin-dependent kinase 5 is an upstream regulator of mitochondrial fission during neuronal apoptosis

K Meuer^{1,4}, IE Suppanz², P Lingor^{1,4}, V Planchamp^{1,4}, B Göricke^{1,4}, L Fichtner^{3,4}, GH Braus^{3,4}, GPH Dietz^{1,4}, S Jakobs², M Bähr^{*1,4} and JH Weishaupt^{1,4}

Under physiological conditions, mitochondrial morphology dynamically shifts between a punctuate appearance and tubular networks. However, little is known about upstream signal transduction pathways that regulate mitochondrial morphology. We show that mitochondrial fission is a very early and kinetically invariant event during neuronal cell death, which causally contributes to cytochrome *c* release and neuronal apoptosis. Using a small molecule CDK5 inhibitor, as well as a dominant-negative CDK5 mutant and RNAi knockdown experiments, we identified CDK5 as an upstream signalling kinase that regulates mitochondrial fission during apoptosis of neurons. Vice versa, our study shows that mitochondrial fission is a modulator contributing to CDK5-mediated neurotoxicity. Thereby, we provide a link that allows integration of CDK5 into established neuronal apoptosis pathways.

Cell Death and Differentiation (2007) 14, 651–661. doi:10.1038/sj.cdd.4402087; published online 12 January 2007

Mitochondria can acquire a broad range of morphologies, from a punctuate shape to a tubular appearance or even extended networks. Several proteins, most of them belonging to the family of large GTPases, have been identified that energy-dependently regulate mitochondrial morphology and subcellular distribution by promoting either fission (Fis1, dynamin-related protein 1 (Drp1), MTP18) or fusion of mitochondria (Mfn1/2 and Opa1).^{1–3} As a potential upstream regulatory factor, the actin cytoskeleton has been shown to be a prerequisite for mitochondrial fission, possibly by its influence on Drp1 recruitment to mitochondria.⁴

Apoptotic release of the mitochondrial cytochrome *c* and other proapoptotic mitochondrial proteins results in formation of the so-called apoptosome, which in turn activates downstream effector caspases with death executing function.⁵ This intrinsic, mitochondrial death pathway is relevant for most forms of neuronal apoptosis, in contrast to extrinsic, for example death receptor mediated, activation of programmed cell death.⁶ However, despite the contribution of mitochondrial dysfunction specifically to the demise of neurons, there is only scarce knowledge about mitochondrial fission during neuronal apoptosis, nor about its functional contribution to neuronal cell death. Furthermore, little is known about upstream regulatory pathways for mitochondrial morphology in general.

Cyclin-dependent kinase 5 (CDK5) is a member of the CDK family, but, distinct from other CDKs, it does not participate in cell cycle regulation.⁷ Instead, CDK5 is physiologically implicated in cytoskeletal functions, as well as regulation of membrane turnover and morphology, for example cell migration or endocytosis. Moreover, it is involved in neuron-

specific functions including, for example, synaptic plasticity, axonal outgrowth or transmitter release.^{8–11} In neurological diseases, deregulated CDK5 turned out to be an apical instigator of neuronal cell death cascades. Amyloid-toxicity was shown to induce calpain-mediated cleavage of the CDK5 activators p35 or p39 to p25 and p29. This leads to redistribution and overactivation of CDK5 after its association with p25/p29.^{12,13} Similarly, deregulation of CDK5, as well as neuroprotection by CDK5 inhibition, was demonstrated in many other models for neuronal cell death.^{14–17}

CDK5 acts early in the cell death cascade before the onset of mitochondrial dysfunction, and CDK5 inhibition prevents the decline of the mitochondrial transmembrane potential.¹⁶ However, CDK5 does not directly translocate to mitochondria,¹⁶ and it remained largely unclear how CDK5 deregulation can be integrated into longer-established 'classical' mitochondrial cell death pathways.

We delineate CDK5 as an upstream regulator of mitochondrial fission. The change in mitochondrial shape takes place within minutes, and with a similar time course independent of the proapoptotic stimulus. We give evidence that mitochondrial scission is necessary for neuronal apoptosis, and show that it contributes to CDK5 neurotoxicity. Thereby, we provide a link between CDK5 deregulation and mitochondrial apoptosis pathways.

Results

Early mitochondrial fission is necessary for neuronal apoptosis. Neuronally differentiated dopaminergic CSM14.1

¹Department of Neurology, University Hospital Göttingen, Göttingen, Germany; ²Mitochondrial Structure and Dynamics Group, Department NanoBiophotonics, Max-Planck-Institute for Biophysical Chemistry, Am Fassberg, Göttingen, Germany; ³Institute for Microbiology and Genetics, University of Göttingen, Grisebachstraße, Göttingen, Germany and ⁴DFG Research Center of the Molecular Physiology of the Brain (CMPB)

*Corresponding author: M Bähr, Department of Neurology, University Hospital Göttingen, Robert-Koch-Str. 40, 37075 Göttingen, Germany. Tel: + 49 551 39 6603; Fax: + 49 551 39 14302; E-mail: mbaehr@gwdg.de

Keywords: mitochondrial fission; neuroprotection; cyclin-dependent kinase; neuronal apoptosis; cyclin-dependent kinase inhibitors; neurodegeneration

Abbreviations: CDK5, cyclin-dependent kinase 5; dCSM cells, neuronally differentiated CSM14.1 cells; Drp1, dynamin-related protein 1; dnDrp1, dominant-negative mutant of dynamin-related protein 1; MPP⁺, 1-methyl-4-phenylpyridinium ion

Received 01.3.06; revised 11.10.06; accepted 08.11.06; Edited by M Piacentini; published online 12.1.07

cells (dCSM cells; see also material and methods) and cultured rat primary midbrain neurons were transfected with the fluorescent protein dsRed2 fused to a mitochondrial targeting signal (mito-dsRed2). This resulted in a fluorescent mitochondria-specific labelling, showing that the vast majority of neuronal cells contained tubular or interconnected mitochondria under control conditions (Figure 1a; Supplementary Figure 1a). Time-course of mitochondrial morphology after apoptosis induction was then studied by time-lapse microscopy. Several cell death inducing agents were tested: Staurosporine, 1-methyl-4-phenylpyridinium ion (MPP⁺), which is the active metabolite of the neurotoxin MPTP used for *in vivo* Parkinson's disease models, and the calcium ionophore A23187. A rapid decline in mean mitochondrial length was observed in dCSM cells within minutes after cell death induction (Figure 1a and b). Moreover, the decay of mitochondrial length followed very similar kinetics, independent of the proapoptotic stimulus, and was similarly found also in rat primary neuronal midbrain cultures (Figure 1a and b). Time-lapse analysis of individual mitochondria confirmed that the observed decrease in mean mitochondrial length was due to mitochondrial fission events, and not caused by shortening or contraction of individual mitochondria (see also Supplementary movie available online on *Cell Death and Differentiation* web site). Demonstrating the specific involvement of the mitochondrial fission machinery, mitochondrial fission was antagonized by co-transfection of a dominant-negative mutant of the mitochondrial fission protein Drp1 (Drp1_{K38A}, tagged with ECFP; Figure 1b).

Our videomicroscopy data were confirmed by counting the proportion of cells that displayed mitochondrial fragmentation (defined by at least 50% punctuate mitochondria), as in dCSM cells we observed a several fold increase in neuronal cells with fragmented mitochondria already 30 min after proapoptotic treatment (Supplementary Figure 1c), that could be attenuated by Drp1_{K38A}. Moreover, similar findings were made with primary neuronal midbrain cultures (Supplementary Figure 1d).

Showing a functional contribution of mitochondrial fission to neuronal apoptosis cascades, we found that the fission inhibiting Drp1_{K38A}-ECFP substantially reduced staurosporine-induced cell death of both dCSM cells (Figure 1c) and rat primary midbrain neurons (Figure 1d). However, although

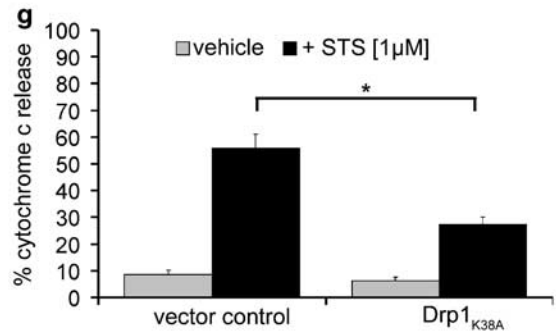
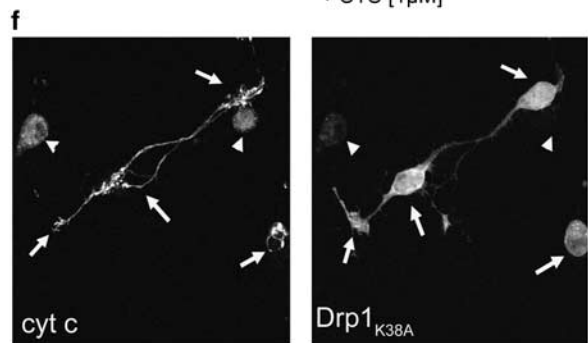
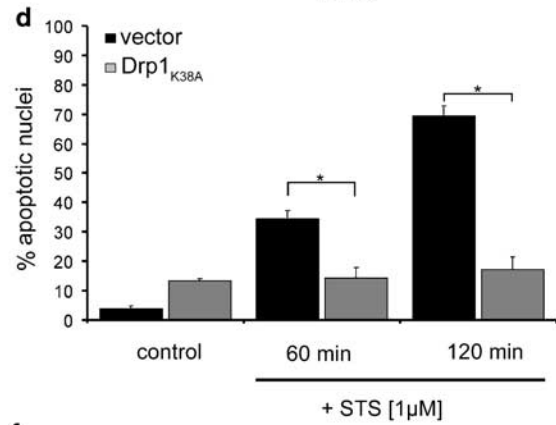
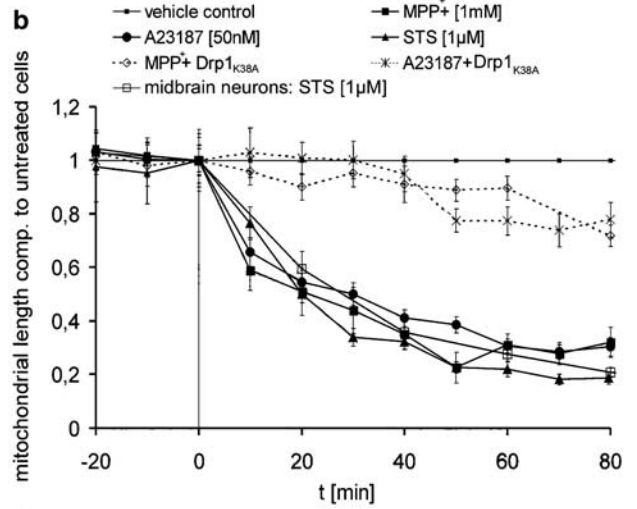
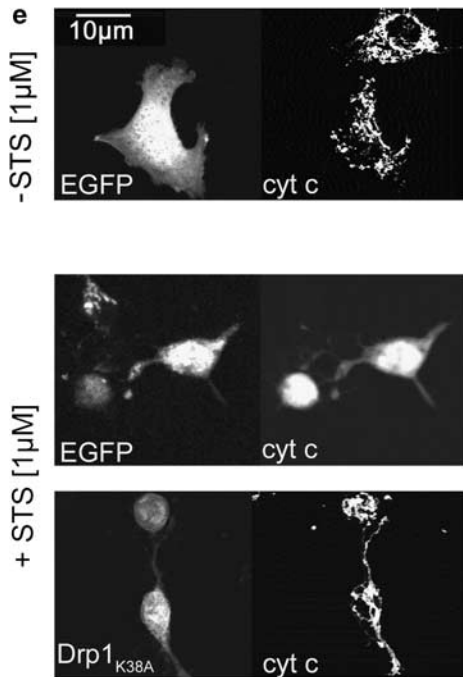
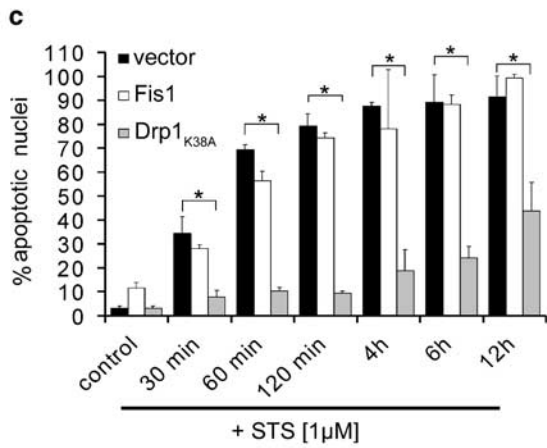
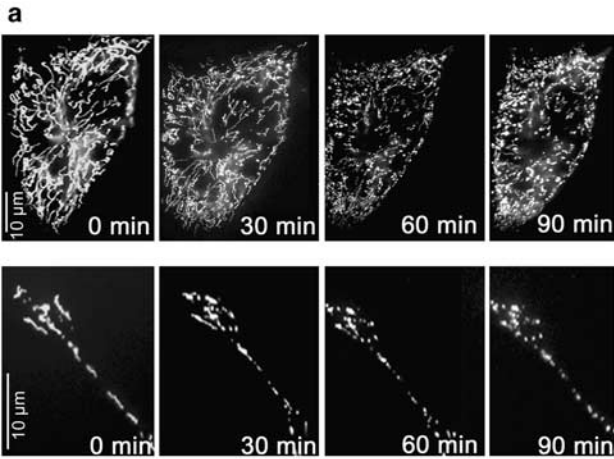
necessary for neuronal cell death, mitochondrial fission was not sufficient to induce apoptosis, as expression of Fis1-EGFP resulted only in marginal cell death (about 10%) without proapoptotic treatment, and did not increase the sensitivity of dCSM cells to staurosporine-induced apoptosis (Figure 1c), regardless of more than 90% Fis1-induced mitochondrial fission within 24 h after transfection (Supplementary Figure 1c).

Nuclear condensation and fragmentation are observed in the final execution phase of neuronal cell death. Thus, we asked whether Drp1_{K38A} would influence the release of mitochondrial cytochrome *c*, a hallmark of the earlier mitochondrial phase of apoptosis. To be able to judge cytochrome *c* distribution within single dCSM cells, we performed immunocytochemistry using an antibody directed against cytochrome *c*. While cytochrome *c* immunoreactivity was clearly confined to a mitochondrial distribution in most control neurons, it changed to a diffuse cytoplasmic pattern when staurosporine was added (Figure 1e–g), which was clearly prevented by Drp1_{K38A}-ECFP expression (Figure 1e–g).

Similar to Drp1_{K38A}, the Bcl-2 protein family member Bcl-xL also interferes with apoptotic cytochrome *c* release and has strong anti-apoptotic effects in neurons, acting at the level of mitochondria.¹⁸ We thus compared Bcl-xL with Drp1_{K38A}, and asked whether Bcl-xL might, directly or indirectly, have similar effects on mitochondrial morphology as well. dCSM cells were treated with recombinant Bcl-xL fused to a Tat protein transduction domain (Tat-Bcl-xL), which is delivered intracellularly and acts anti-apoptotically as shown before.¹⁹ Despite the expected anti-apoptotic effect and prevention of cytochrome *c* release (Figure 2a and b), Tat-Bcl-xL did not alter mitochondrial morphology (Figure 2c), suggesting that Bcl-xL acted downstream or in parallel to the mitochondrial fission machinery. This finding demonstrates that preventing mitochondrial dysfunction is not sufficient to prevent mitochondrial fission.

CDK5 induces caspase-independent mitochondrial fission. The search for cellular functions upstream of apoptotic mitochondrial fission in neurons was the primary aim of our study. Parts of the mitochondrial fission machinery colocalizes with cytoskeletal structures, and translocation of

Figure 1 . Early mitochondrial fission is necessary for neuronal apoptosis. In order to stain mitochondria, neuronally differentiated CSM cells (dCSM cells) or rat primary midbrain neurons were transfected with mitochondrially targeted dsRed2. (a) Time-lapse videomicroscopy showing mitochondrial fragmentation in a representative dCSM cell upon MPP⁺ treatment (upper panels), or a neuron in primary neuronal midbrain cultures upon STS treatment (1 μM; lower panels). (b) Quantification of time-lapse videomicroscopy reveals mitochondrial fission starting within minutes after treatment with staurosporine, MPP⁺ or the calcium ionophore A23187. Kinetics of mitochondrial fragmentation was found to be very similar independent of the proapoptotic stimulus. Fragmentation was attenuated by overexpression of Drp1_{K38A}-ECFP (Drp1_{K38A}). In (b), mitochondrial length was standardized to values of untreated control cells. (c, d) Staurosporine treatment (STS; 1 μM) for up to 12 h induced nuclear fragmentation (DAPI staining). Cotransfection with Drp1_{K38A}-ECFP prevented nuclear signs of apoptosis. Apoptosis was quantified at the indicated time points after staurosporine treatment as percentage of transfected cells with pyknotic or fragmented nuclei. Drp1_{K38A}-ECFP protected both staurosporine-treated dCSM cells (c) and cultured primary midbrain neurons (d). (e–g) Drp1_{K38A}-ECFP prevents apoptotic cytochrome *c* release in neurons. Neuronal dCSM cells were stained with a cytochrome *c* antibody and a Cy3-coupled secondary antibody. Cytochrome *c* immunoreactivity was clearly confined to a mitochondrial distribution in most control cells (e; upper panel). After staurosporine treatment (STS), a change in cytochrome *c* staining to a diffuse pattern was observed (e, middle panel), which was prevented by Drp1_{K38A}-ECFP expression (e, lower panel). Almost all staurosporine-treated cells expressing Drp1_{K38A}-ECFP after transient transfection (arrows in f, right panel) displayed a mitochondrial cytochrome *c* distribution (visible in the Cy3 channel shown in the left panel of e; arrows), while lack of Drp1_{K38A}-ECFP expression was always accompanied by cytochrome *c* release in the same culture well (f, arrowheads). (g) Quantification of staurosporine-induced cytochrome *c* release in transfected dCSM cells, which is significantly reduced by Drp1_{K38A}-ECFP expression. Expression of the fluorophore-tagged Drp1_{K38A} (Drp1_{K38A}-ECFP) was verified by respective fluorescence for each cell included in the analysis. Control cells were transfected with EGFP only. (*): *P* < 0.05 as determined by ANOVA followed by Student–Newman–Keuls test (b) or two-tailed Student's *t*-test (c, d, g)



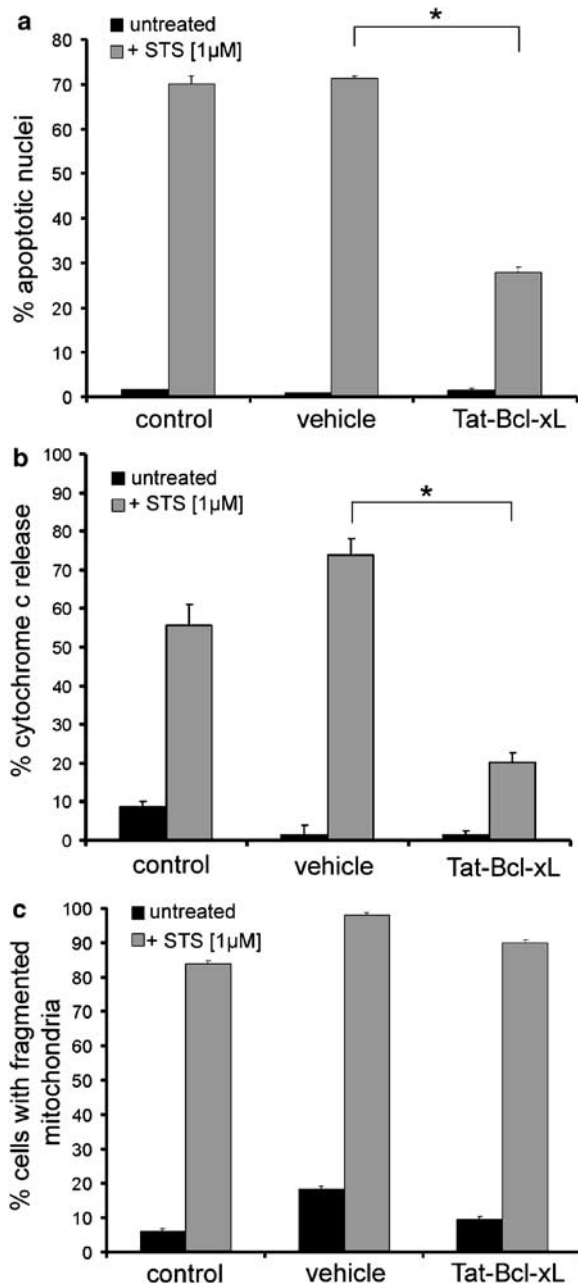


Figure 2 Bcl-xL is neuroprotective, but does not influence mitochondrial fission. Staurosporine-treated ($1 \mu\text{M}$ for 2 h) dCSM cell cultures had a significantly increased proportion of cells with apoptotic nucleus (a), released cytochrome c (b; determined by cytochrome c immunohistochemistry as in Figure 1) as well as cells with predominantly fragmented mitochondria (c). Concomitant treatment with the cell permeable Tat-Bcl-xL fusion protein protected from staurosporine-induced cell death and cytochrome c release (a, b; $P < 0.05$ compared to staurosporine exposure alone; two-tailed Student's *t*-test), but did not prevent mitochondrial fragmentation in staurosporine-challenged cultures (c). Control: untreated or only staurosporine-treated, respectively. Vehicle: Addition of Tat-Bcl-xL elution buffer was used as vehicle control. $n = 3$ independent experiments

Drp1 to mitochondria seems to be actin-dependent.^{20,4} CDK5 is known to contribute to the regulation of the actin and tubulin cytoskeleton, as well as regulation of membrane turnover and morphology, for example cell migration or

endocytosis.^{8–10} Altogether, this led us to hypothesize that CDK5, which is an upstream instigator of neuronal demise in various neuronal cell death models, might participate in a signal transduction pathway that links proapoptotic signals to the dynamic changes of mitochondrial morphology we had observed.

Consequently, we co-transfected dCSM cells and primary midbrain neurons with EGFP-tagged CDK5 and p25 or p35. P25 is the toxic proteolytic product of the physiological CDK5 activator p35, which results in overactivation and subcellular redistribution of CDK5.

Supporting our hypothesis of an involvement of CDK5 in the regulation of mitochondrial fission, overexpression of p35/CDK5, and even more pronounced expression of p25/CDK5, was sufficient to induce mitochondrial fragmentation both in dCSM cells and cultured primary midbrain neurons (Figure 3a–c). Moreover, p25/CDK5-induced mitochondrial fission depended on the above described fission machinery, because co-expression of the dominant-negatively acting Drp1_{K38A}-EGFP abolished p25/CDK5-induced mitochondrial fission, both in neuronal dCSM cells and primary neuronal midbrain cultures (Figure 3a–c). As expected based on its known neurotoxic effect, p25/CDK5 expression, induced apoptosis in transfected cells, which could also be suppressed by co-transfection with Drp1_{K38A}-EGFP (Figure 3d and e).

CDK5 initiates neuronal apoptosis cascades, including activation of caspases, of which most are acting downstream of mitochondrial dysfunction. As expected, the pan-caspase inhibitor zVAD-fmk blocked CDK5-initiated apoptosis (Figure 3d). However, the mitochondrial fission promoting effect of p25/CDK5 was not significantly reduced by caspase inhibition, demonstrating that the pro-fission effect of CDK5 is not mediated by caspases (Figure 3b), and general anti-apoptotic treatments do not prevent mitochondrial fission.

Staurosporine- and A23187-induced mitochondrial fission is CDK5-dependent. We next asked whether CDK5 also contributes to mitochondrial fission when cell death is not induced by direct upregulation of CDK5 activity as in the experiments described above, but by other apoptotic stimuli that induce mitochondrial fission. Before investigating this question using the staurosporine-treated dCSM cells, we verified that CDK5 indeed contributed to cell death in staurosporine-induced apoptosis of dCSM cells. We confirmed that CDK5 and one of its neuronal activators, p39, were expressed in dCSM cells as assessed by Western blot analysis (data not shown). CDK5 activity measured by a CDK5 kinase assay^{16,12} increased upon staurosporine treatment (Figure 4a). Moreover, expression of a dominant-negatively acting CDK5 mutant (CDK5_{N144}-EGFP), or treatment with the highly potent CDK5 inhibitor indolinone A¹⁶ blocked cell death (Figure 4b) as well as caspase3/7 activation (Figure 4c).

Analysis of non-apoptotic control cultures did not reveal a significant effect of CDK5 inhibition on mean mitochondrial length in dCSM cells. Mean mitochondrial length was 2.33 ± 0.15 , 2.01 ± 0.10 and $2.00 \pm 0.18 \mu\text{m}$ in control-transfected cells or cells transfected with wild-type CDK5-EGFP or CDK5_{N144}-EGFP, respectively. As a positive control, Drp1_{K38A}-EGFP was transfected, which resulted in a

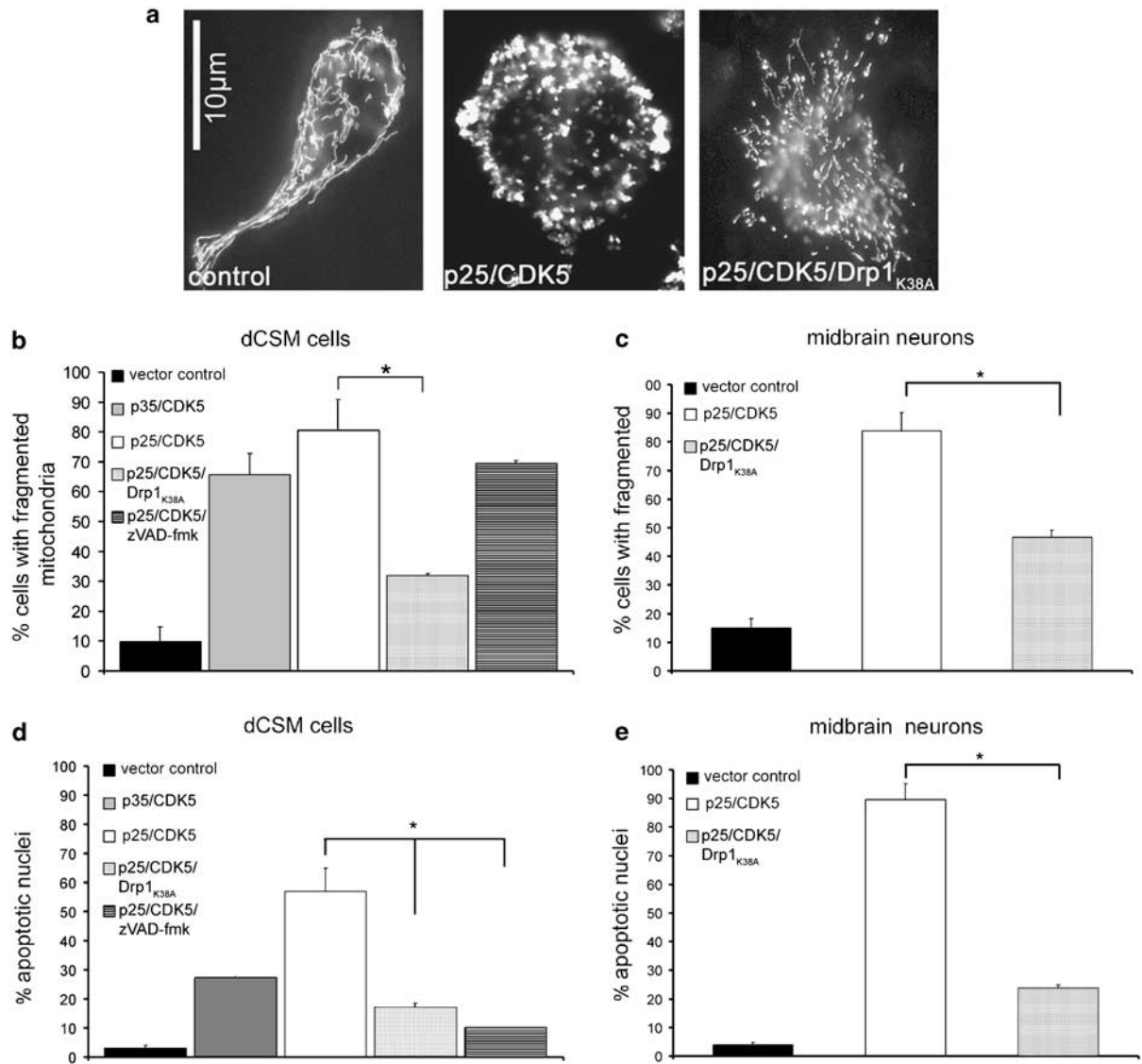


Figure 3 Overexpression of p25/CDK5 is sufficient to induce mitochondrial fragmentation in a caspase-independent manner. Overexpression of EGFP-tagged CDK5/p25 resulted in mitochondrial fission in most transfected cells after 18 h (a–c), both in dCSM cells (a, b) and cultured primary midbrain neurons (c). Additional overexpression of Drp1_{K38A}-EGFP blocked this effect (a–c). (Co-) expression of the fluorophore-tagged proteins was verified by respective fluorescence for each cell included in the analysis. (d, e) As expected, p25/CDK5 overexpression induced cell death in dCSM cells (d) and primary neuronal midbrain cultures (e) 18 h after transfection, which was also substantially attenuated by Drp1_{K38A}-EGFP. The pan-caspase inhibitor zVAD-fmk blocked CDK5-mediated apoptosis (d), but not mitochondrial fission (b). (*): $P < 0.05$; two-tailed Student's *t*-test

significantly increased mean mitochondrial length of $3.48 \pm 0.21 \mu\text{m}$ (100 mitochondria from 10 cells per condition analysed).

In contrast to healthy cells, we observed a strong effect of CDK5 inhibition on mitochondrial morphology under apoptotic conditions. Treatment with the highly specific CDK5 small molecule inhibitor indolinone A (250 nM) reduced staurosporine-induced mitochondrial fission compared to cultures that were treated with staurosporine alone (Figure 5a).

Moreover, serial live cell images (Figure 5b and c) as well as blinded counting of the proportion of cells that displayed predominantly punctuate mitochondria (Figure 5d) confirmed that indolinone A substantially diminished mitochondrial fission after both staurosporine and A23187 treatment. The

same effect could be observed in cells that expressed the dominant-negative CDK5 mutant CDK5N₁₄₄-EGFP (Figure 5e and f). Similarly, staurosporine-induced mitochondrial fission that was observed in live rat primary midbrain neurons was attenuated by CDK5N₁₄₄ expression, with an even more pronounced effect compared to dCSM cells (Figure 5g).

Moreover, we found additional evidence that the effect of CDK5 on mitochondrial fission is mediated by modulation of the known fission machinery: co-expression of wild-type Drp1-EGFP antagonized the reduction of mitochondrial fission under indolinone A treatment or CDK5N₁₄₄-EGFP expression (Figure 5b, d–f). Concomitantly, downstream anti-apoptotic effects of CDK5 inhibition could also be reversed by Drp1 expression: We found a reduced proportion of cells with

apoptotic nuclei or released cytochrome *c* in cells treated with indolinone A or expressing CDK5N₁₄₄-EGFP (Figure 6a–c). Again, this effect was abolished by overexpression of wild-

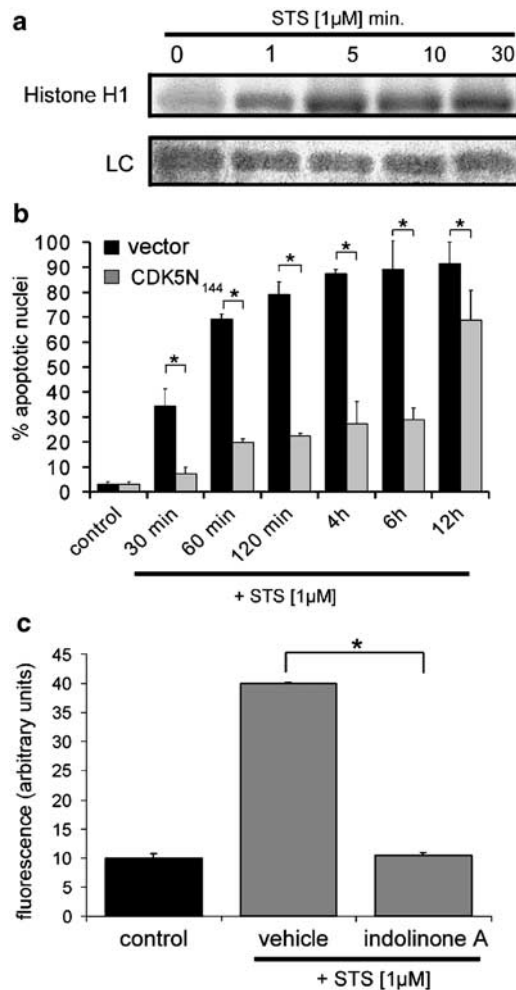


Figure 4 CDK5 activity is involved in staurosporine-induced death of dCSM cells. (a) Staurosporine treatment induced an early transient increase in CDK5 activity in neuronal dCSM cells. Histone H1 was used as CDK5 substrate. LC: Loading control demonstrating equal amounts of CDK5 protein. The loading control was performed by Coomassie staining of the same SDS gel that was subsequently used for autoradiographic detection of CDK5 activity (see Materials and methods). Staurosporine-induced cell death (b) and caspase-3/7 activity (c) could be blocked by a dominant-negative CDK5 mutant (CDK5N₁₄₄-EGFP) or the CDK5 inhibitor indolinone A (250 nM), respectively. In (b), the percentage of cells with apoptotic nuclei refers to the population of CDK5N₁₄₄-EGFP transfected cells. (*): $P < 0.05$; two-tailed Student's *t*-test

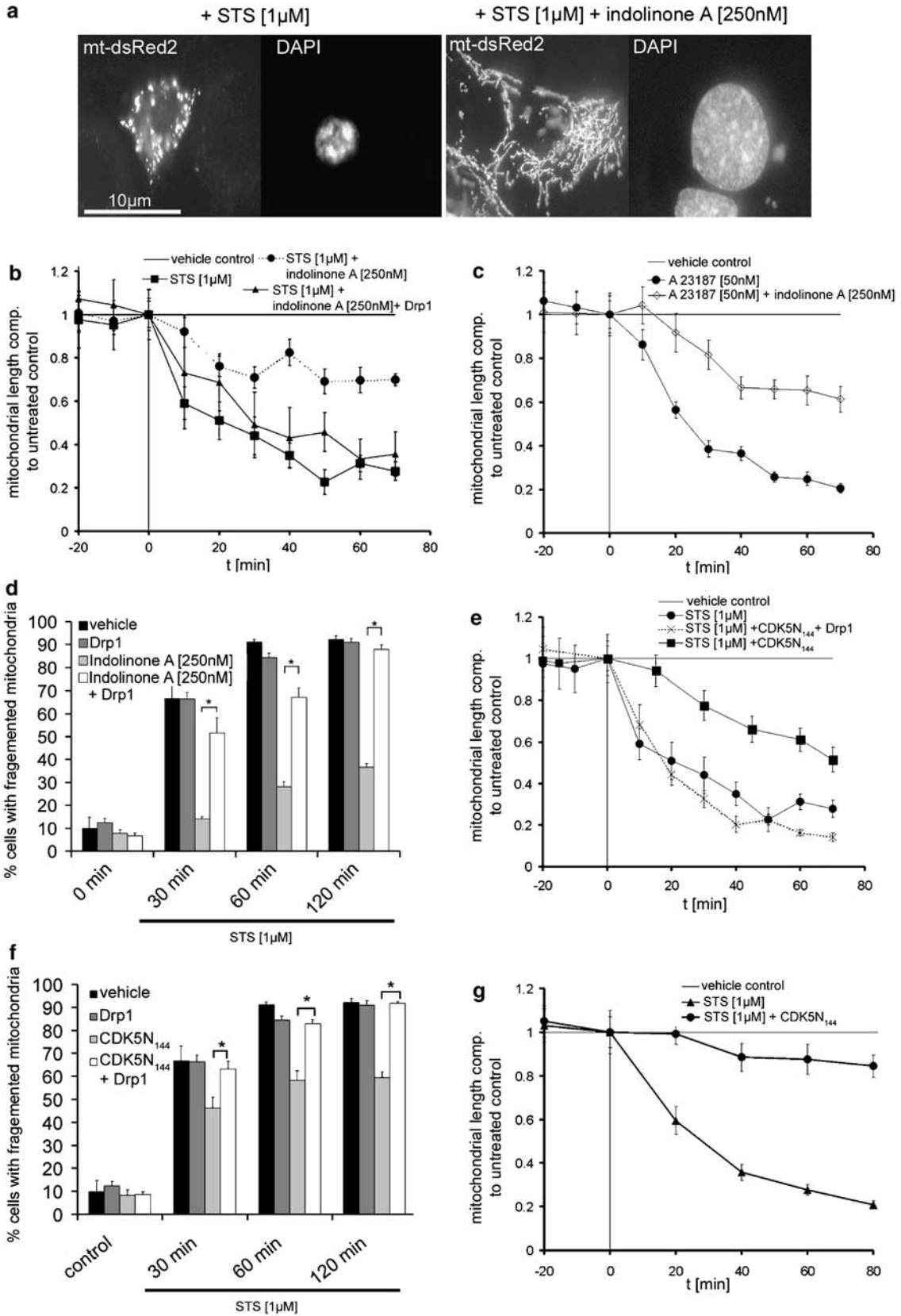
Figure 5 Inhibition of CDK5 attenuates apoptotic mitochondrial fragmentation. (a) Treatment with the CDK5 inhibitor indolinone A prevents mitochondrial fragmentation upon staurosporine-treatment (STS). dCSM cells were treated with STS for 2 h (1 μ M; left panels). Right panels show preserved mitochondrial fragmentation under concomitant treatment with indolinone A (250 nM). Note that the CDK5 inhibitor did also prevent apoptotic nuclear condensation as shown by DAPI labelling. (b, c) Quantitative time-lapse microscopy confirmed that indolinone A (250 nM) reduced staurosporine- (b) or A23187-induced (c) mitochondrial fission. The effect of indolinone A could be antagonized by co-expression with wild-type Drp1 (b). Mitochondrial length was standardized to untreated control cells. (d) The effect of indolinone A was confirmed by blinded counting of cells displaying predominantly punctuate mitochondria. Indolinone A reduced the percentage of dCSM cells with fragmented mitochondria at different time points after staurosporine treatment, which was again antagonized by co-expression with wild-type Drp1. (e, f) Effects comparable to indolinone A treatment were observed in cells expressing the dominant-negative CDK5 mutant CDK5N₁₄₄-EGFP (e: time-lapse microscopy; f: blinded counting of cells with fragmented mitochondria). Also here, the effect of CDK5N₁₄₄ could be antagonized by co-expression with wild-type Drp1 (Drp1; Drp1-ECFP). Note that Drp1 expression did not induce mitochondrial fragmentation by itself. (Co-) expression of CDK5N₁₄₄-EGFP and Drp1-ECFP protein was verified by EGFP and ECFP fluorescence for each cell included in the analysis. (g) Similar to the results obtained in the neuronal dCSM cells, staurosporine-induced mitochondrial fission of cultured primary midbrain neurons was inhibited by CDK5N₁₄₄-EGFP, as shown by quantification of time-lapse microscopy data. (*): $P < 0.05$ as determined by ANOVA followed by Student–Newman–Keuls test (b, c, g) or two tailed student's *t* test (d, f)

type Drp1. It is important to note that wild-type Drp1 did not induce mitochondrial fission or apoptosis when expressed alone, confirming previous data in non-neuronal mammalian cells.¹

CDK5 knockdown reduces mitochondrial fission. In the concentration applied in our experiments, Indolinone A is a highly specific CDK5 inhibitor.¹⁶ Moreover, our data were confirmed by the parallel use of a dominant-negative CDK5 mutant. Nevertheless, an unspecific effect of indolinone A or dnCDK5 on kinases other than CDK5 cannot be completely excluded, although identical results from the small molecule CDK5 inhibitor and the dominant-negative CDK5 mutant make artefacts by unspecific co-inhibition of other kinases extremely unlikely. However, in order to further strengthen the central claim of our study, we performed CDK5 knockdown experiments using RNAi. Confirming our previous results, knockdown of CDK5 protein by RNAi (Figure 7a) clearly attenuated apoptotic mitochondrial fission (Figure 7b). Moreover, reminiscent of our data obtained with CDK5 RNAi in neuronal cells, a yeast deletion strain lacking *pho85*, the yeast orthologue of CDK5, displayed a reduced proportion of fragmented mitochondria (Supplementary Figure 2).

Discussion

In a systematic time-course analysis, we found that mitochondrial fragmentation occurred early during neuronal apoptosis, and was largely invariant, regardless of the fission-inducing stimulus. This is reminiscent of the constant time period required for complete apoptotic cytochrome *c* release, which is independent of the mode or strength of the apoptotic stimulus.²¹ Most likely, both mitochondrial fission and release of mitochondrial cytochrome *c* are basic mechanisms of cell death with conserved, invariant time dynamics. Our findings in apoptotic models are in line with one earlier report that describes mitochondrial fission in neurons exposed to excitotoxic conditions.²² Consistent with few recent studies that demonstrated the relevance of mitochondrial fission for apoptosis of non-neuronal mitotic cells^{23–26} our study provides evidence that mitochondrial fission is not a mere epiphenomenon of neuronal cell death, but that blocking mitochondrial fission is indeed protective for neurons. However, our data obtained from Fis1-EGFP overexpression exemplify that induction of mitochondrial fission, although necessary, is not sufficient to induce apoptosis. Similarly, experiments using Bcl-xL showed that apoptosis can at least



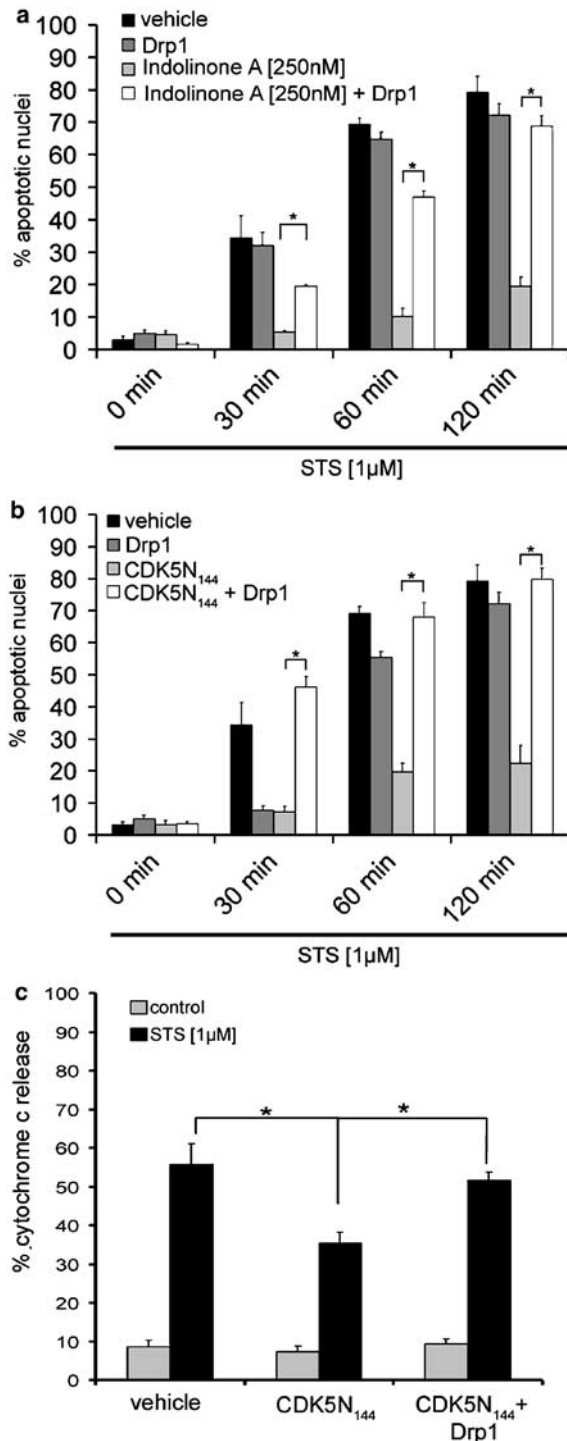


Figure 6 Neuroprotective effects of CDK5 inhibition are reversed by Drp1. Indolinone A treatment (a) or CDK5N₁₄₄-EGFP expression (b) prevented nuclear signs of apoptosis at different time points after staurosporine treatment. This effect could be antagonized by co-expression of wild-type Drp1. Importantly, Drp1 did not induce apoptosis by itself. (c) CDK5N₁₄₄-EGFP expression suppressed cytochrome c release in dCSM cells after 2 h staurosporine exposure (STS; 1 μM). This effect was abolished by co-expression of wild-type Drp1. Percentage values represent the proportion of cells with diffuse cytoplasmic cytochrome c staining compared to cells with labeling restricted to mitochondria (see also Figure 2). (*): $P < 0.05$; two tailed students *t*-test

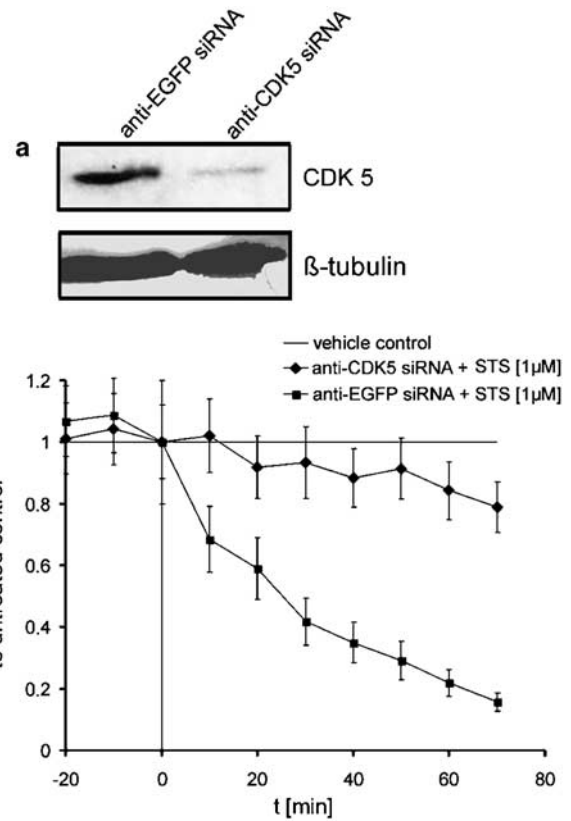


Figure 7 (a) Western blot demonstrating specific downregulation of the endogenous CDK5 protein. dCSM cells were transfected with 33 nM anti-CDK5 siRNA or for control condition with 33 nM anti-EGFP siRNA. At 3 days after transfection cells were lysed and Western blots were performed. All lanes were loaded with the same amount of total protein as indicated by β-tubulin detection. (b) Quantification of time-lapse microscopy shows mitochondrial fragmentation induced by staurosporine treatment (1 μM) is prevented by CDK5 siRNA. Mitochondrial length was standardized to untreated control cells

temporarily be blocked without preventing mitochondrial fission.

After we had shown the requirement of mitochondrial fission for neuronal apoptosis, we proceeded to study the involvement of CDK5 in apoptotic mitochondrial fission, the main focus of our study. Disruption of the actin cytoskeleton precludes mitochondrial fission in non-neuronal cell lines⁴ and neurons (our unpublished observation). The findings of an implication of cytoskeletal proteins in mitochondrial fission prompted us to examine whether CDK5 was a modulator of mitochondrial fission in neurons. CDK5 is an apical instigator in many neuronal cell death cascades^{15,14,27,17} and phosphorylates various proteins implicated in cytoskeletal organization.^{28,29} In addition, CDK5 has previously been shown to be implicated in various cellular events involving turnover of biological membranes, for example cell migration, axonal outgrowth or endocytosis.^{10,27,11} These cellular functions also require cytoskeletal structures, and we considered that, albeit a simplifying view, the process of mitochondrial fission shares mechanistic similarities with the cleavage of cell membranes during 'pinching off' of endocytotic vesicles.

Although it is known that CDK5 acts upstream of mitochondrial dysfunction in neuronal cell death paradigms,¹⁶

it remained unclear how CDK5 could be conceptually integrated in established mitochondrial cell death cascades. Our data not only delineate the first signal transduction kinase regulating cell death-associated mitochondrial fission in mammalian cells, but also link CDK5 to 'classical' apoptosis pathways with mitochondrial disintegration and subsequent cytochrome *c* release.

We have not identified here the direct substrate of CDK5 that is relevant for mitochondrial fission. The pivotal direct CDK5 targets to induce mitochondrial fission could well be among already known CDK5 substrates, possibly including components of the cytoskeleton. In our study, we show that the effect of CDK5 is at least partially mediated via the known fission protein Drp1, implicating the mitochondrial fission machinery in the observed changes in mitochondrial morphology. Intriguingly, CDK5 has previously been demonstrated to play a critical role in synaptic vesicle endocytosis by phosphorylation of dynamin 1.¹¹ Similarly, the dynamin-related protein 1 (Drp1) may be directly modulated by CDK5. However, CDK5 could also indirectly regulate Drp1 function or localization by phosphorylation of one or several other CDK5 substrates, for example via cytoskeletal alterations.

Furthermore, reduced mitochondrial fission under CDK5 inhibitory treatment cannot be explained as a secondary effect due to general preservation of mitochondrial function. Supporting this view, the anti-apoptotic protein Bcl-xL, despite its well-established protective effects at the mitochondrial level, does not prevent mitochondrial fission (James *et al.* this study). In contrast to Bcl-xL, Bcl-2 was shown to block mitochondrial fission.³⁰ However, in this case a direct interaction of Bcl-2 with the fission machinery, and not the general preservation of mitochondrial functions, was shown to be responsible for the reduction in mitochondrial fission.³⁰ Finally, we found that caspase-inhibition with a pan-caspase inhibitor prevented cell death, but not mitochondrial fission induced by p25/CDK5. This further excludes unspecific effects of anti-apoptotic treatments on mitochondrial fission, and shows that CDK5-induced fission is caspase-independent.

In principle, increased fusion instead of decreased fission could explain the effect of CDK5 inhibition on mitochondrial shape. However, the effect of CDK5 both on mitochondrial shape and on apoptosis was mediated via the mitochondrial fission protein Drp1. As Drp1 is only involved in mitochondrial fission, but not in fusion, we can conclude that the protective effects of CDK5 inhibition are mediated via the mitochondrial fission machinery.

Based on our current knowledge, it is possible that apart from CDK5 additional upstream signal transduction pathways may also contribute to the regulation of apoptotic mitochondrial fission in neurons. Vice versa, depending on the cell death paradigm, additional mechanisms other than mitochondrial fission are likely to contribute to CDK5 toxicity. For instance, nuclear translocation of CDK5 and a nuclear pathway leading to inactivation of the protective transcription factor MEF2 by nuclear CDK5 has recently been described.³¹ Accordingly, nuclear CDK5 toxicity could have at least contributed to CDK5-mediated cell death in our paradigm, although inhibition of specifically nuclear CDK5 activity was

protective in excitotoxic cell death, but not, for example, in the purely apoptotic model of camptothecin-induced neuronal cell death.³¹ Moreover, while the EGFP tag itself results in partial nuclear localization of respective fusion proteins, we never observed an increase in nuclear EGFP-tagged CDK5 or p25 in our paradigm, and always noted a substantial degree of cytoplasmic localization for both proteins (data not shown). The fact that also the only cytoplasmically localized p35/CDK5 resulted in mitochondrial fission is in agreement with the cytoplasmic CDK5 activity directly influencing mitochondrial morphology. However, this does not conflict with concepts of nuclear mechanisms of CDK5 toxicity, for example inactivation of the transcription factor MEF2, as both effects may contribute to neuronal cell death at the same time.

The observation that also the cytosolic physiological p35/CDK5 resulted in mitochondrial fragmentation suggests that p35/CDK5 activity may also contribute to mitochondrial fission occurring under several physiological circumstances which are not accompanied by p25 generation and cell death, for example during cell cycle.

Similar to our observations on CDK5 inhibition in neurons, lack of its orthologue Pho85⁴⁰ resulted in less fragmented mitochondria in *Saccharomyces cerevisiae*. Our findings are principally intriguing in light of the conserved functions of Pho85/CDK5 that have been identified so far: similar to CDK5, Pho85 contributes to organization of the actin cytoskeleton in yeast,^{32,33} and plays a role in the cellular stress response.^{34,35} The fact that CDK5 inhibition and Pho85 deletion resulted in parallel effects on mitochondrial morphology could be an indication for at least partially conserved kinase pathways modulating mitochondrial morphology. However, despite principally similar effects on mitochondrial morphology, one also has to emphasize that there are profound differences between yeast and higher eukaryotes, for example concerning their cytoskeleton.

Recapitulating, we show that mitochondrial fragmentation is necessary for neuronal apoptosis and takes place within minutes after induction of apoptosis with similar kinetics, independent of the type of proapoptotic treatment. We identified CDK5 as a signal transduction kinase modulating mitochondrial fission, integrating CDK5 into established neuronal apoptosis pathways. Vice versa, we show that mitochondrial fission is required and a mediator for neurotoxic CDK5 action, although basal p35/CDK5 activity may also contribute to mitochondrial fission under physiological circumstances. Thus, our study contributes to the understanding of CDK5 action in neuronal cell death cascades, but also highlights the mitochondrial fission machinery as a potential target for therapeutic approaches against neurodegenerative diseases.

Materials and Methods

Chemical reagents. Cell culture reagents were purchased from PAA Laboratories. Staurosporine, nocodazole and MPP⁺ were obtained from Sigma-Aldrich (Cölbe, Germany), A23187 from Alexis (Grünberg, Germany). Z-VAD-FMK were obtained from Bachem (Weil am Rhein). Indolinone A was provided by Boehringer Ingelheim Pharma KG, Ingelheim, Germany.

Expression vectors and Tat-Bcl-xL fusion protein. Expression plasmids for mito-dsRed2 and EGFP-N₂ were purchased from Clontech, hFis1-EGFP and Drp1_{K38A}-ECFP were kind gifts from J-C Martinou, constructs for

CDK5N₁₄₄-EGFP and p25-EGFP were generously provided by L-H Tsai. Tat-Bcl-xL was expressed and the fusion protein purified as described previously.¹⁹

Cell culture and transfection. CSM14.1 cells are derived from the ventral mesencephalic region of an E14 rat, and immortalized with the temperature-sensitive Large T antigen.³⁶ When cultured at 33°C (permissive temperature), CSM14.1 cells express the large T antigen, proliferate, have a flat neuroepithelial-like morphology and express the neural stem cell marker nestin.³⁶ When transferred to 39°C, the temperature-sensitive large T antigen is inactivated and proliferation ceases. Moreover, CSM14.1 cells acquire a neuron-like morphology, extend neurites, and differentiate into neuronal cells expressing the dopaminergic markers Nurr1, TH and ALDH2. Grafted differentiated CSM14.1 cells have been successfully used to alleviate symptoms in hemiparkinsonian animals.³⁷ For our study, CSM14.1 cells were cultured and differentiated for 6–8 weeks in complete DMEM supplemented with 10% heat-inactivated fetal calf serum, 100 U/ml penicillin and streptomycin at 39°C in 5% CO₂ (called dCSM cells in this paper).

For time-lapse microscopy and cell death assays, dCSM cells were grown in 0.8 cm² chamber slides (eight-well Lab-Tek chambered cover glass system; Nalgene Nunc, Naperville, IL). Cells (2×10^6 per well) were transfected with plasmid DNA using the Amaxa electroporation system according to the manufacturer's instructions (kit primary neurons, program 0-03).

Mitochondria were visualized by transfection with mito-dsRed2. Co-labelling with the small molecule mitochondrial stain mitotracker green confirmed the specific mitochondrial distribution of the dsRed2 (data not shown). As CDK5N₁₄₄, Drp1_{K38A}, p25 or Fis1 were fluorophore-tagged (ECFP or EGFP), we cotransfected EGFP along with mito-dsRed2 in control conditions. 24 h after transfection respective compounds were applied at the following concentrations: 1 μ M staurosporine, 50 nM A23187, 1 mM MPP⁺, 250 nM indolinone A and 500 nM Tat-Bcl-xL.

siRNA transfection. Anti-CDK5 siRNA was chemically synthesized by Qiagen (Hilden, Germany) and Cy3 conjugated at the 5' end. The following sequence was used: anti-CDK5-sense 5' GAG GAU CUU UCG ACU GCU A-3', anti-CDK5-antisense 5' UAG CAG UCG AAA GAU CCU C-3'. Anti-EGFP siRNA was also chemically synthesized by Qiagen (Hilden, Germany) and had the following sequences: anti-EGFP-sense 5' GCA AGC UGA CCC UGA AGU UCA U-3', anti-EGFP-antisense 5' GAA CUU CAG GGU CAG CUU GCC G-3'. Anti-EGFP siRNA was used as a control. Lyophilized siRNA was reconstituted following the manufacturer's instructions. For targeting of endogenous genes by cationic lipid-mediated transfection, siRNA was complexed with Lipofectamine 2000 (Invitrogen, Karlsruhe, Germany) according to manufacturer's instructions. Per well of a 24-well culture plate, 1 μ l Lipofectamine 2000 was diluted in 50 μ l Opti-Mem[®] I Reduced serum medium and combine with 20 pmol siRNA (resulting in a final concentration of 33 nM) diluted in 50 μ l Opti-Mem[®] I Reduced serum medium after 5 min of incubation at room temperature. The formulation was continued for 20 min at room temperature and the mixture was applied to the culture wells. Three days after transfection protein lysates for Western blot analysis or time lapse videomicroscopy were performed.

Western blot analysis. For preparation of protein lysates, dCSM14.1 were plated on six-well plates. After 80–90% confluence was reached, cells were lysed in lysis buffer¹⁶ on ice for 15 min, and cell debris was pelleted at 13 000 *g* for 30 min. Western blotting was performed as described earlier.¹⁶ CDK5 (C-8) and p35 (C-19) antibodies (both rabbit) were purchased from Santa Cruz. P39 antibody (polyclonal, rabbit) was kindly provided by L-H Tsai.

Primary midbrain neuron cultures and transfection. The mesencephalic floor plate was dissected from E14 Wistar rat embryos and further processed for establishing dissociated cell cultures as previously described.³⁸ For DNA transfection, cell pellets consisting of 2×10^6 cells each were resuspended in electroporation medium (Amaxa biosystems; Frankfurt) and 2 μ g of plasmid DNA was added to the solution. The primary neuron solution was then transfected using the Nucleofector device (Amaxa biosystems; Frankfurt) according to manufacturer's instructions. Transfected cells were seeded on poly-L-ornithine/laminin (Sigma)-coated eight-well chamber slides at a density of 175 000 cells/cm². Cultures were maintained at 37°C in a humidified atmosphere and 5% CO₂ in DMEM/F12 plus the N1 supplements and antibiotics for 2–4 days. Neurons were identified by their typical morphology and axonal processes.

Analysis of mitochondrial fragmentation in neurons. Eight-well chamber slides that allow the parallel imaging of four separately transfected cell populations of the same preparation and under identical experimental condition were used throughout the study. At 24 h after transfection and at least 30 min before application of cell death inductors (staurosporine, MPP⁺, A23187) time-lapse images were collected at intervals of 1–15 min. Cells were incubated in a microscope climate chamber for live cell imaging (37°C, 5% CO₂) on a Zeiss Axioplan inverted microscope (Carl Zeiss). A 63 \times 1.4 NA oil immersion objective (Carl Zeiss) was used, and images captured using a CCD camera (Carl Zeiss).

Mitochondrial length was measured using Axiovision software. At least 15 randomly chosen mitochondria per cell from different cytoplasmic regions were measured in μ m, and then standardized to and given as percentage compared to untreated control cells. Data were obtained from time-lapse videomicroscopic pictures of at least 5–10 cells from different preparations per condition. In further experiments, mitochondria of fixed cells were scored as normal (tubular, elongated) or fragmented (> 50% of the mitochondria in a given cell appeared punctuate), and results expressed as percentage of cells with predominantly fragmented mitochondria.

Cell death assay. At 24 h after transfection with respective expression plasmids cells were treated with staurosporine (1 μ M) and fixed with 4% paraformaldehyde/PBS. For experiments using Tat-Bcl-xL, cells were preincubated for 2 h with Tat-Bcl-xL before induction of cell death. For experiments using zVAD-fmk (100 μ M), cells were preincubated over night with zVAD-fmk before induction of cell death. Nuclei were stained with DAPI and imaged with a Zeiss fluorescent microscope. Cells were scored as normal or apoptotic (i.e. pyknotic or fragmented) nuclei. At least 200 transfected cells from at least 3 independent wells per condition were counted and values calculated as percentage of cells with apoptotic nuclei compared total cell counts.

CDK5 activity assay. dCSM14.1 were plated on 15 cm dishes. After 80–90% confluence was reached, cells were incubated with staurosporine [1 μ M] for 1, 5, 10, 30 min. After incubation with staurosporine cells were lysed in lysis buffer on ice for 15 min, and cell debris was pelleted at 13 000 *g* for 30 min. 50% bead slurry (30 μ l) were added to 500 μ g of protein lysate for 1 h at 4°C to remove proteins unspecifically binding to the beads. The beads were then collected by centrifugation, the pellet was discarded and the supernatant was incubated with 10 μ l of CDK5 (Santa Cruz, C-8) antibody for 1 h at 4°C followed by incubation with another 30 μ l beads. The beads were collected by centrifugation and washed three times with lysis buffer and three times with kinase buffer (10 mM MgCl₂, 50 mM Hepes, 1 mM DTT, 1 μ M ATP). Washed beads were incubated with 10 μ g histone H1 (Sigma, Steinberg, Germany). The reaction was initiated at 30°C after addition of ³²P-labeled γ -ATP (Amersham, Uppsala, Sweden), allowed to proceed for 30 min at RT, and stopped by addition of sample buffer and heating to 95°C for 5 min. After SDS-PAGE, gels were fixed with 40% (v/v) ethanol, 10% (v/v) acetic acid for 60 min. After two washing steps with water for 10 min, gels were stained with 80% colloidal coomassie (0.1% (w/v) Coomassie Brilliant Blue G250, 2% (w/v) ortho-phosphoric acid, 10% (w/v) ammoniumsulfat) and 20% (v/v) methanol for 1 h at RT. Gels were destained in 1% (v/v) acetic acid, dried and subjected to Phosphorimager-analysis.

Immunocytochemistry. Cells grown on glass coverslips were fixed with 4% paraformaldehyde/PBS and subsequently permeabilized with 0.1% Triton X-100 for 20 min. To block unspecific immunoreactivity, cells were then incubated with PBS containing 5% NGS and 1% BSA for 30 min. Anti-cytochrome *c* mouse monoclonal antibody (PharMingen) was used at 1 : 1000 dilution in PBS. The secondary Cy3-labelled antibody was obtained from Dianova and used at 1 : 1000 dilution.

Analysis of mitochondrial fragmentation in yeast. Growth and manipulation of yeast was carried out according to standard procedures. The wild-type strain BY4741 and the isogenic *pho85* deletion strain were obtained from Euroscarf (Frankfurt, Germany). The disruption was confirmed by polymerase chain reaction.

To label the mitochondrial matrix with GFP, the cells were transformed with the plasmid pVT100U-mtGFP.³⁹ Cells were grown in SC medium with 2% glucose at 30°C to logarithmic growth phase. For imaging and phenotypic analysis cells were chemically fixed in 10% formaldehyde for 10 min. Mitochondrial phenotypes were counted in blinded experiments by two observers. Each experiment, comprising more than 100 analyzed cells per strain, was repeated at least six times.

Statistical analysis. All values are expressed as mean \pm S.E.M. The two-sided *t*-test, or ANOVA followed by Student–Newman–Keuls test was used to determine significance as appropriate (NCSS Software, NCSS, Kaysville, Utah).

Acknowledgements. We thank Jean-Claude Martinou and Manuel Rojo for the gift of Fis1 and Drp1 plasmids, and Pawel Kermer for CSM14.1 cells. p25, p35 and CDK5 constructs as well as p39 antibody were generously provided by Li-Huei Tsai. We also thank Christine Poser for excellent technical assistance. We thank Stefan W Hell for his continuous support (SJ). Funded by Deutsche Forschungsgemeinschaft through the DFG-Research Center for Molecular Physiology of the Brain.

- James DI, Parone PA, Mattenberger Y, Martinou JC. hFis1, a novel component of the mammalian mitochondrial fission machinery. *J Biol Chem* 2003; **278**: 36373–36379.
- Bossy-Wetzel E, Barsoum MJ, Godzik A, Schwarzenbacher R, Lipton SA. Mitochondrial fission in apoptosis, neurodegeneration and aging. *Curr Opin Cell Biol* 2003; **15**: 706–716.
- Tondera D, Czaderna F, Paulick K, Schwarzer R, Kaufmann J, Santel A. The mitochondrial protein MTP18 contributes to mitochondrial fission in mammalian cells. *J Cell Sci* 2005; **118**: 3049–3059.
- De Vos KJ, Allan VJ, Grierson AJ, Sheetz MP. Mitochondrial function and actin regulate dynamin-related protein 1-dependent mitochondrial fission. *Curr Biol* 2005; **15**: 678–683.
- Desagher S, Martinou JC. Mitochondria as the central control point of apoptosis. *Trends Cell Biol* 2000; **10**: 369–377.
- Yoshida H, Kong YY, Yoshida R, Elia AJ, Hakem A, Hakem R *et al*. Apaf1 is required for mitochondrial pathways of apoptosis and brain development. *Cell* 1998; **94**: 739–750.
- van den Heuvel S, Harlow E. Distinct roles for cyclin-dependent kinases in cell cycle control. *Science* 1993; **262**: 2050–2054.
- Nikolic M, Dudek H, Kwon YT, Ramos YF, Tsai LH. The cdk5/p35 kinase is essential for neurite outgrowth during neuronal differentiation. *Genes Dev* 1996; **10**: 816–825.
- Chae T, Kwon YT, Bronson R, Dikkes P, Li E, Tsai LH. Mice lacking p35, a neuronal specific activator of Cdk5, display cortical lamination defects, seizures, and adult lethality. *Neuron* 1997; **18**: 29–42.
- Zukerberg LR, Patrick GN, Nikolic M, Humbert S, Wu CL, Lanier LM *et al*. Cables links Cdk5 and c-Abl and facilitates Cdk5 tyrosine phosphorylation, kinase upregulation, and neurite outgrowth. *Neuron* 2000; **26**: 633–646.
- Tan TC, Valova VA, Malladi CS, Graham ME, Berven LA, Jupp OJ *et al*. Cdk5 is essential for synaptic vesicle endocytosis. *Nat Cell Biol* 2003; **5**: 701–710.
- Patrick GN, Zukerberg L, Nikolic M, de La MS, Dikkes P, Tsai LH. Conversion of p35 to p25 deregulates Cdk5 activity and promotes neurodegeneration. *Nature* 1999; **402**: 615–622.
- Patzke H, Tsai LH. Calpain-mediated cleavage of the cyclin-dependent kinase-5 activator p39 to p29. *J Biol Chem* 2002; **277**: 8054–8060.
- Nguyen MD, Lariviere RC, Julien JP. Deregulation of Cdk5 in a mouse model of ALS: toxicity alleviated by perikaryal neurofilament inclusions. *Neuron* 2001; **30**: 135–147.
- Osuga H, Osuga S, Wang F, Fetni R, Hogan MJ, Slack RS *et al*. Cyclin-dependent kinases as a therapeutic target for stroke. *Proc Natl Acad Sci USA* 2000; **97**: 10254–10259.
- Weishaupt JH, Kussmaul L, Grottsch P, Heckel A, Rohde G, Romig H *et al*. Inhibition of CDK5 is protective in necrotic and apoptotic paradigms of neuronal cell death and prevents mitochondrial dysfunction. *Mol Cell Neurosci* 2003; **24**: 489–502.
- Smith PD, Crocker SJ, Jackson-Lewis V, Jordan-Sciutto KL, Hayley S, Mount MP *et al*. Cyclin-dependent kinase 5 is a mediator of dopaminergic neuron loss in a mouse model of Parkinson's disease. *Proc Natl Acad Sci USA* 2003; **100**: 13650–13655.
- Parsadanian AS, Cheng Y, Keller-Peck CR, Holtzman DM, Snider WD. Bcl-xL is an antiapoptotic regulator for postnatal CNS neurons. *J Neurosci* 1998; **18**: 1009–1019.
- Dietz GP, Kilic E, Bahr M. Inhibition of neuronal apoptosis *in vitro* and *in vivo* using TAT-mediated protein transduction. *Mol Cell Neurosci* 2002; **21**: 29–37.
- Varadi A, Johnson-Cadwell LI, Cirulli V, Yoon Y, Allan VJ, Rutter GA. Cytoplasmic dynein regulates the subcellular distribution of mitochondria by controlling the recruitment of the fission factor dynamin-related protein-1. *J Cell Sci* 2004; **117**: 4389–4400.
- Goldstein JC, Waterhouse NJ, Juin P, Evan GI, Green DR. The coordinate release of cytochrome *c* during apoptosis is rapid, complete and kinetically invariant. *Nat Cell Biol* 2000; **2**: 156–162.
- Rintoul GL, Filiano AJ, Brocard JB, Kress GJ, Reynolds IJ. Glutamate decreases mitochondrial size and movement in primary forebrain neurons. *J Neurosci* 2003; **23**: 7881–7888.
- Frank S, Gaume B, Bergmann-Leitner ES, Leitner WW, Robert EG, Catez F *et al*. The role of dynamin-related protein 1, a mediator of mitochondrial fission, in apoptosis. *Dev Cell* 2001; **1**: 515–525.
- Lee YJ, Jeong SY, Karbowski M, Smith CL, Youle RJ. Roles of the mammalian mitochondrial fission and fusion mediators Fis1, Drp1, and Opa1 in apoptosis. *Mol Biol Cell* 2004; **15**: 5001–5011.
- Jagasia R, Grote P, Westermann B, Conrad B. DRP-1-mediated mitochondrial fragmentation during EGL-1-induced cell death in *C. elegans*. *Nature* 2005; **433**: 754–760.
- Arnout D, Rismanchi N, Grodet A, Roberts RG, Seeburg DP, Estaquier J *et al*. Bax/Bak-dependent release of DDP/TIMM8a promotes Drp1-mediated mitochondrial fission and mitoptosis during programmed cell death. *Curr Biol* 2005; **15**: 2112–2118.
- Dhavan R, Tsai LH. A decade of CDK5. *Nat Rev Mol Cell Biol* 2001; **2**: 749–759.
- Feng Y, Walsh CA. Protein–protein interactions, cytoskeletal regulation and neuronal migration. *Nat Rev Neurosci* 2001; **2**: 408–416.
- Rashid T, Banerjee M, Nikolic M. Phosphorylation of Pak1 by the p35/Cdk5 kinase affects neuronal morphology. *J Biol Chem* 2001; **276**: 49043–49052.
- Kong D, Xu L, Yu Y, Zhu W, Andrews DW, Yoon Y *et al*. Regulation of Ca²⁺-induced permeability transition by Bcl-2 is antagonized by Drp1 and hFis1. *Mol Cell Biochem* 2005; **272**: 187–199.
- O'Hare MJ, Kushwaha N, Zhang Y, Aleyasin H, Callaghan SM, Slack RS *et al*. Differential roles of nuclear and cytoplasmic cyclin-dependent kinase 5 in apoptotic and excitotoxic neuronal death. *J Neurosci* 2005; **25**: 8954–8966.
- Huang D, Patrick G, Moffat J, Tsai LH, Andrews B. Mammalian Cdk5 is a functional homologue of the budding yeast Pho85 cyclin-dependent protein kinase. *Proc Natl Acad Sci USA* 1999; **96**: 14445–14450.
- Lee J, Colwill K, Anelinas V, Tennyson C, Moore L, Ho Y *et al*. Interaction of yeast Rvs167 and Pho85 cyclin-dependent kinase complexes may link the cell cycle to the actin cytoskeleton. *Curr Biol* 1998; **8**: 1310–1321.
- Huang D, Moffat J, Andrews B. Dissection of a complex phenotype by functional genomics reveals roles for the yeast cyclin-dependent protein kinase Pho85 in stress adaptation and cell integrity. *Mol Cell Biol* 2002; **22**: 5076–5088.
- Gillardon F, Schratzenholz A, Sommer B. Investigating the neuroprotective mechanism of action of a CDK5 inhibitor by phosphoproteome analysis. *J Cell Biochem* 2005; **95**: 817–826.
- Haas SJ, Wree A. Dopaminergic differentiation of the Nurr1-expressing immortalized mesencephalic cell line CSM14.1 *in vitro*. *J Anat* 2002; **201**: 61–69.
- Anton R, Kordower JH, Kane DJ, Markham CH, Bredesen DE. Neural transplantation of cells expressing the anti-apoptotic gene bcl-2. *Cell Transplant* 1995; **4**: 49–54.
- Lingor P, Unsicker K, Kriegstein K. GDNF and NT-4 protect midbrain dopaminergic neurons from toxic damage by iron and nitric oxide. *Exp Neurol* 2000; **163**: 55–62.
- Westermann B, Neupert W. Mitochondria-targeted green fluorescent proteins: convenient tools for the study of organelle biogenesis in *Saccharomyces cerevisiae*. *Yeast* 2000; **16**: 1421–1427.
- Nishizawa M, Kanaya Y, Toh E. Mouse cyclin-dependent kinase (Cdk) 5 is a functional homologue of a yeast Cdk, pho85 kinase. *J Biol Chem* 1999; **274**: 33859–33862.

Supplementary Information accompanies the paper on Cell Death and Differentiation website (<http://www.nature.com/cdd>)